

# The effect of waveguide open end modification on acoustic wave attenuation

Łukasz GORAZD 🕞

AGH University of Krakow, al. A. Mickiewicza 30, 30-059 Kraków

Corresponding author: Łukasz GORAZD, email: gorazd@agh.edu.pl

**Abstract** The work presents experimental research on the possibility of attenuation acoustic wave radiation through the waveguide open end without flow, depending on its modification. One of the methods of noise protection is a modification consisting in changing the outlet impedance by applying a various types of acoustic systems. The work focused on determining the outlet impedance of a waveguide outlet with a modified geometry in the plane wave range using the transfer function method. A measurement setup was constructed on which measurements were performed analogously to those in an impedance tube. The measurement setup was verified based on the measurements of the reference sample as well as theoretical and numerical calculations. The results of experimental studies of parameters related to acoustic wave attenuation for different variants of open-end waveguide modifications are presented.

**Keywords:** duct termination, transfer function method, duct acoustics, acoustic impedance.

## 1. Introduction

The acoustic wave propagating inside the channels and then emitted through the waveguide outlet can constitute a significant nuisance, mainly in duct systems found in industry. These include, among others, heating, ventilation and air conditioning systems (HVAC). Modification of the waveguide outlet geometry is an important issue due to the modification of the acoustic pressure field distribution. Information about the actual attenuation of the acoustic wave can be obtained by determining the outlet impedance. Analytical solutions apply only to some cases involving the waveguide outlet, such as a waveguide with a constant cross-section ending with an outlet truncated perpendicular to the waveguide axis [1-5]. The analytical solution of the radiation wave through the waveguide end placed in an infinite flange is also well described in the literature [2, 6]. More complicated cases in terms of the waveguide outlet geometry can be obtained using numerical methods [7-10], e.g. the finite element method (FEM) or boundary element method (BEM) or others [11, 12], as well as by carrying out acoustic measurements [13]. The most common way to minimize noise propagating in a waveguide is to use muffler. Reflective mufflers are characterized by good attenuation properties in the low and medium frequency range. Reflective mufflers works on the principle of reflection and interference of acoustic waves as a result of the appearance of discontinuities in the channel, the acoustic impedance of which is significantly greater or smaller than the acoustic impedance of the waveguide. They are generally used where high flow rates and high temperatures occur (e.g. combustion engines, blowers, compressors). Absorption mufflers enable attenuation of acoustic waves in the medium and high frequency range (e.g. ventilation ducts). An alternative to porous materials are microperforated materials with a perforation diameter in the range of 0.5-1 mm, which can be used to make a fragment of a waveguide placed in a housing to form an muffler [14].

The work focused on determining the outlet impedance of a waveguide with a modified geometry in the plane wave range using the transfer function method (TF). The modification of the outlet is related to changing the duct open end by attaching a fragment of a waveguide constituting e.g. a muffler, or a fragment of such structure at the end, etc. The measurement setup and the theoretical basis for determining the outlet impedance based on the reflection coefficient for various variants of waveguide open end modification are presented. The influence of a flange placed at the end of the outlet was also examined.

In Section 2 transfer function method for determining the reflection coefficient and acoustic impedance of a waveguide outlet and basic assumptions are described, together with its main theoretical formulae. Section 3 contains descriptions of the experimental measurements, the most important parameters of the measurement set-up. Section 4 contains a descriptions of the experimental measurements variants. Section

5 presents final result of the reflection coefficient, outlet impedance and comparison with theoretical and numerical calculations.

## 2. Theoretical foundations

In analytical considerations, assumptions are most often made related to the geometry of the problem (semi-infinite waveguide or infinite waveguide, infinite flange, constant cross-section), boundary conditions, medium parameters and sound sources. It was assumed that only a plane wave can propagate inside a hard-walled waveguide. In the case of a change in impedance along the propagation path of the wave, the acoustic wave is reflected, and its amplitude depends on the reflection coefficient *R* 

$$p_r(x,t) = R \cdot p_i = R \cdot A_0 e^{i(\omega t + kx)}, \tag{1}$$

where  $p_i$  – acoustic pressure of incident wave,  $p_r$  – acoustic pressure of reflected wave,  $A_0$  – amplitude of incident wave, R – reflection coefficient,  $\omega = 2\pi f$  – angular frequency, x – coordinate in space,  $k = \frac{\omega}{c}$  – wave number

Impedance is expressed by the ratio of the total acoustic pressure  $p = p_i + p_r$  at a given point in the acoustic field to the total acoustic velocity  $v = v_i + v_r$  at that point. The acoustic velocity can be calculated from the one-dimensional Euler equation, taking x as the direction of wave propagation

$$v(x,t) = -\frac{1}{\rho_0} \int \frac{\partial p(x,t)}{\partial x} dt , \qquad (2)$$

where  $\rho_0$  is the density of the medium (for air it is 1.2 kg/m3).

Assuming that the wave reflection occurs at the field point x = 0, the impedance can be determined using

$$Z = \frac{p(0,t)}{v(0,t)} = \rho_0 c \frac{(1+R)}{(1-R)},\tag{3}$$

where c is the speed of sound.

For a given value of the reflection coefficient, the sound absorption coefficient can be calculated using formula [15]:

$$\alpha = 1 - |R|^2. \tag{4}$$

The sound pressure level of the wave emitted by the waveguide outlet is also influenced by the radiation impedance  $Z_r$ . Theoretical considerations most often concern the radiation impedance of a cylindrical waveguide end placed in an rigid planar flange [2, 3, 16]. The radiation impedance of a waveguide is analogous to the radiation resistance of a piston. Radiation impedance is a complex quantity whose real part is resistance  $R_z$  and imaginary part is reactance  $R_z$  [2]:

$$Z_{rad} = \rho_0 cS[R_Z(2ka) - iX_Z(2ka)], \qquad (5)$$

where  $S = \pi a^2$  – cross-sectional area of the waveguide outlet with radius a,  $R_Z(x) = 1 - \frac{2J_1(x)}{2x}$  – radiation resistance,  $X_Z(x) = \frac{2H_1(x)}{x}$  – radiation reactance,  $J_V(x)$  – Bessel function of order V,  $H_{\alpha_H}(x)$  – Struve function of order  $\alpha_V$ 

Theoretical considerations of the acoustic wave for the open-ended i.e. unflanged circular tube were described by Levine and Schwinger [17]. In the case of a plane wave, for ka < 1.5 values, approximate formulas can be used [8]:

$$\frac{z_{rad}}{z_c} = ik\delta_0 - i(ka)^3 [0.036 - 0.034 \ln(ka) + 0.0187(ka)^2] + \frac{(ka)^2}{4} + (ka)^4 [0.0127 + 0.082 \ln(ka) - 0.023(ka)^3],$$
(6)

where  $Z_c = \frac{\rho_0 c}{s}$  – characteristic impedance of the pipe,  $\delta_0 = 0.6133a$  – end length correction for an unflanged pipe.

The radiation impedance based on measurements of the transfer function  $H_{12}$  between two microphone positions placed in the waveguide can be determined from the formula [18]:

$$\frac{Z_{rad}}{Z_c} = i \frac{H_{12} \sin(kx_1) - \sin(kx_2)}{\cos(kx_2) - H_{12} \cos(kx_1)},\tag{7}$$

where  $H_{12} = \frac{p_2}{p_1} = \frac{p_i e^{-ikx_2} + p_r e^{ikx_2}}{p_i e^{-ikx_1} + p_r e^{ikx_1}}$  – transfer function between microphones  $p_1$  and  $p_2$  located respectively at distances  $x_1$  and  $x_2$  from the waveguide end (see Figure 1).

## 3. Research methodology and basic assumptions

The measurements were carried out for the waveguide of inner radius  $a=75\,\mathrm{mm}$  shown schematically in the Figure 1. Theoretical considerations are related to determining the reflection coefficient and therefore the impedance of the waveguide termination in a manner analogous to that in an impedance tube based on the transfer function [19]. The reduced frequency of the first Bessel mode (1,1) is ka=1.84, hence, taking into account the assumption of pure plane wave propagation, the upper frequency should not exceed the cut-off frequency of this mode. The upper frequency range was assumed to be 1200 Hz. The distance between the microphones should meet the condition  $s< c/2f_u$  and be less than half the wavelength of the upper frequency range –  $s=0.1\,\mathrm{m}$  was assumed.

The measurements were performed using the generated signal in the frequency range from 50 to 1200 Hz, with a resolution of 1 Hz, with constant amplitude for all spectral components and random phases. The signal recording time was 16 s.

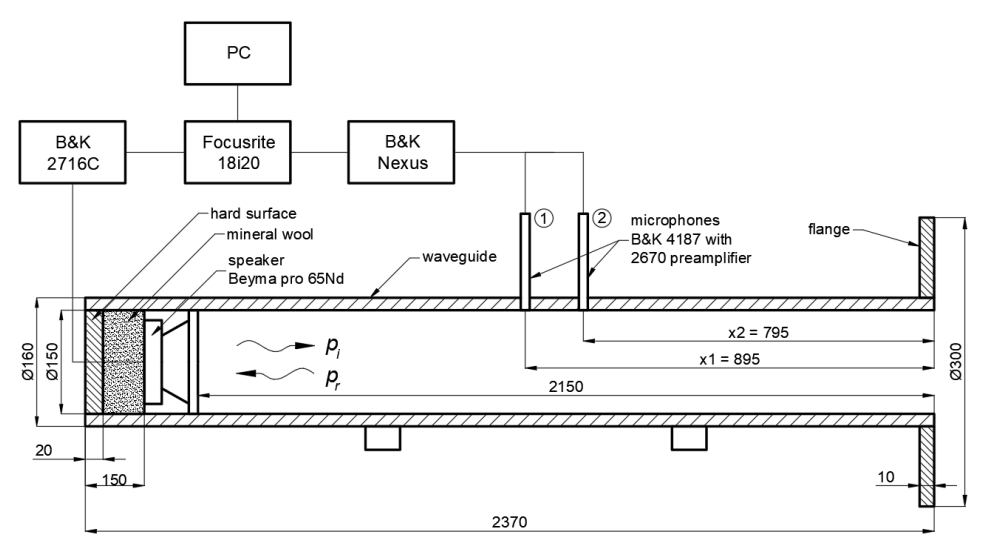


Figure 1. Scheme of the measuring setup (dimensions in mm).

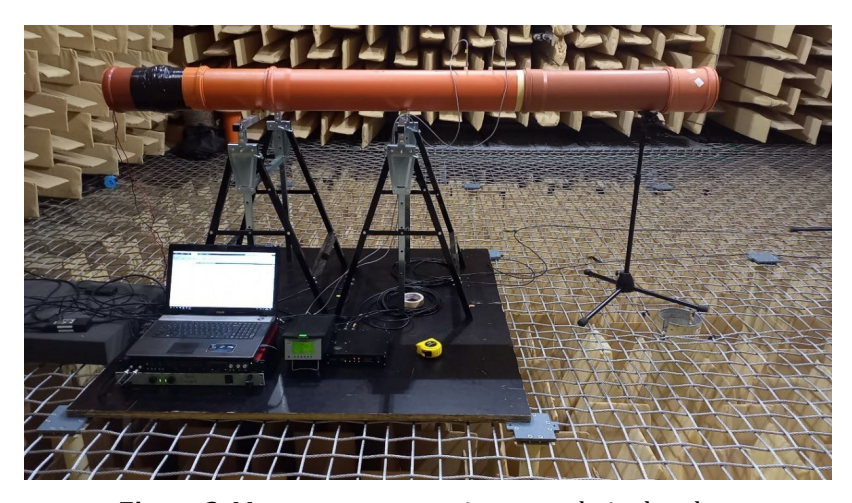


Figure 2. Measurement setup in an anechoic chamber.

The measurements were carried out taking into account a predetermined calibration factor  $H_c$  determined according to [19] by measuring the transfer function between the microphones in their initial (I) and interchanged positions (II). The calibration factor  $H_c$  was determined to compensate the amplitude-phase differences between microphones for the analyzed waveguide terminated with a rigid surface, with

a mineral wool calibration sample placed inside—analogous to the impedance tube. The waveguide was placed in a anechoic chamber

$$H_c = \sqrt{H_{12}^I \cdot H_{12}^{II}} \,. \tag{8}$$

The reflection coefficient for normal incidence of an acoustic wave can be calculated according to equation

$$R = \frac{H_{12c} - e^{iks}}{e^{-iks} - H_{12c}},\tag{9}$$

where  $s = x_1 - x_2$  – distance between microphones,  $H_{12c} = H_{12}/H_c$  – the transfer function corrected for the amplitude and phase mismatch of the microphones.

The measurement setup was verified by measuring the absorption coefficient of a mineral wool sample and comparing it with the results obtained in a B&K 4206T impedance tube. The calibration sample was made of mineral wool with a density of  $\rho_c$  = 36 kg/m³ and dimensions of diameter  $d_c$  = 0.15 m and thickness  $g_c$  = 0.11 m and placed inside a waveguide terminated with a rigid surface.

The presented measurement values (Figure 3) are the average of three measurements obtained with each re-attachment of the sample. The results of the absorption coefficient of the sample used to verify the measuring setup are shown in the Figure 3. The standard deviation of the three measurements obtained for each re-attachment of the sample is shown in the Figure 4.

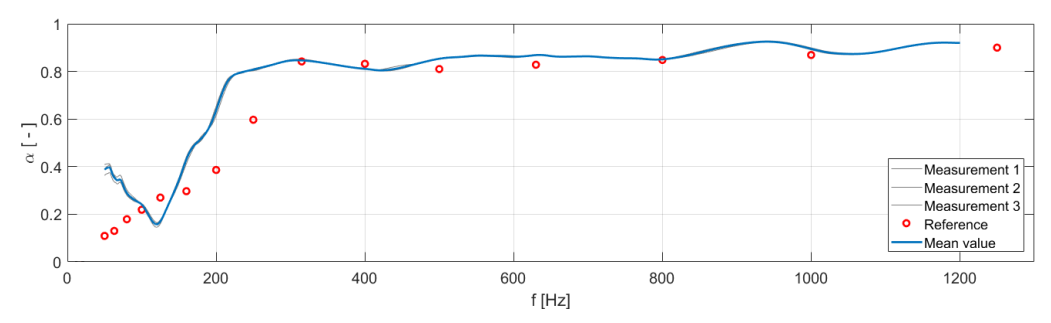


**Figure 3.** Comparison of the absorption coefficient values obtained at the measuring setup (mean value marked by a solid blue line) and in the B&K 4206T impedance tube (reference – marked by red dots).

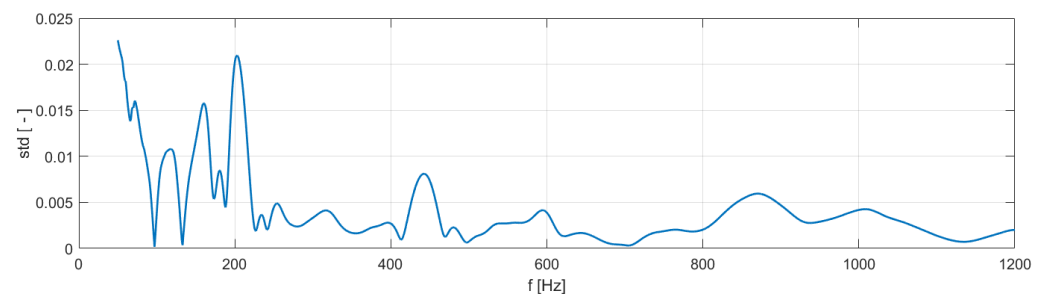


Figure 4. Standard deviation values from three measurements after re-attachment of the sample.

The discrepancies in the measurement results for frequencies below 150 Hz are due to the frequency band transmitted by the Beyma 65Nd loudspeaker. The frequency response of the loudspeaker used in the measurements is in the range of 150 - 8000 Hz. Slight differences between the values measured on the constructed measuring setup and in the B&K 4206T impedance tube, especially for frequencies up to 250 Hz may be due to different mounting conditions and sealing of the sample in the pipe. Low values of standard deviation indicate high repeatability of measurement results at the measuring setup.

In order to determine the difference in the sound pressure level for the individual variants of the waveguide end modification, measurements were performed at an additional point located 1 m from the outlet.

Numerical calculations of the radiation impedance for the flanged and unflanged waveguide outlet were performed using the finite element method (FEM) in Comsol Multiphysics software. The perfectly matched layer (PML) condition was applied to the domain surrounding the waveguide outlet to simulate open boundaries as in a free field. The inner walls of the waveguide were modeled as hard, satisfying the Neumann condition  $-\frac{\partial p}{\partial \rho}\Big|_{\rho=a}=0$ . The obtained results were compared with theoretical and measured values.

# 4. Waveguide outlet modification variants

The waveguide outlet modifications included eight variants. The influence of the flange on the waveguide open end impedance was determined based on measurements, as was the influence of using the other structures shown in Figure 5.

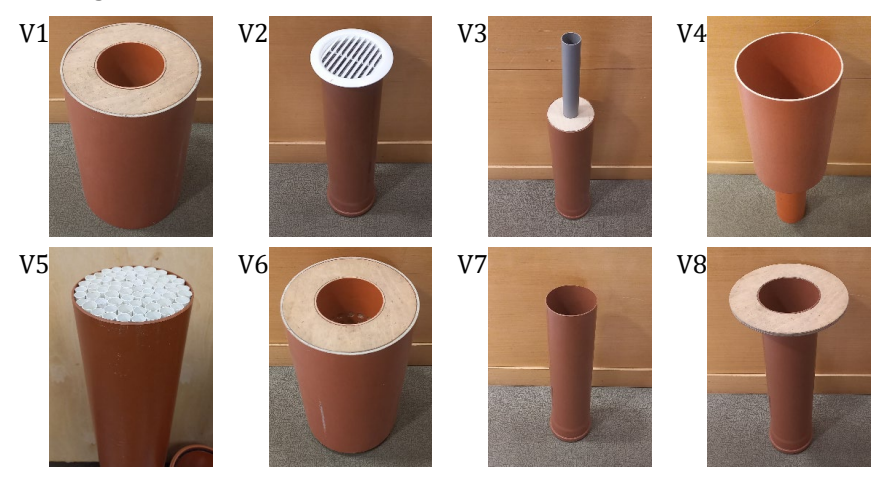


**Figure 5.** Waveguide open end modification variants: V1 – micro-perforated muffler (MPP), V2 – ventilation grille, V3 – sudden contraction, V4 – sudden expansion, V5 – tubes in open end, V6 – absorption muffler, V7 – open end without flange, V8 – open end with flange.

Some of the waveguide outlet end modification variants used during the measurements are described in more detail below.

Variant V1 is a microperforated muffler consisting of a microperforated channel placed in the expansion chamber. The diameter of the holes in this case was  $0.5 \, \text{mm}$ , the perforation ratio coefficient – 1%. The length of the expansion chamber was  $380 \, \text{mm}$  and the microperforation was made over a length of  $215 \, \text{mm}$ .

Variant V3 – The sudden contraction is caused by a sudden change in the waveguide diameter. The acoustic wave is radiated by a tube with an inner diameter of 46 mm and a length of 290 mm.

Variant V4 – Sudden expansion is achieved by placing the outlet in a 300 mm diameter flange together with a 510 mm long housing.

Variant V5 – Inside the waveguide at the outlet, 64 PVC tubes of various lengths with an internal diameter of 16 mm and a wall thickness of 1 mm were randomly placed. The number and length of individual tubes are:  $4 \times 0.32$  m,  $6 \times 0.3$  m,  $8 \times 0.28$  m,  $7 \times 0.26$  m,  $7 \times 0.24$  m,  $8 \times 0.22$  m,  $8 \times 0.20$  m,  $6 \times 0.18$  m,  $10 \times 0.16$  m.

Variant V6 is an absorption muffler consisting of a perforated channel wrapped in mineral wool placed in an expansion chamber. The diameter of the holes in this case was 20 mm, the perforation ratio coefficient was 32%. The length of the expansion chamber was 380 mm, and the perforation was made over a length of 380 mm.

## 5. Results

The effect of the flange on the change of the waveguide open end impedance was investigated (Figure  $6\,a$ ). A comparison of the termination impedance of individual variants (V1-V7) was also presented (Figure  $6\,b$ ).

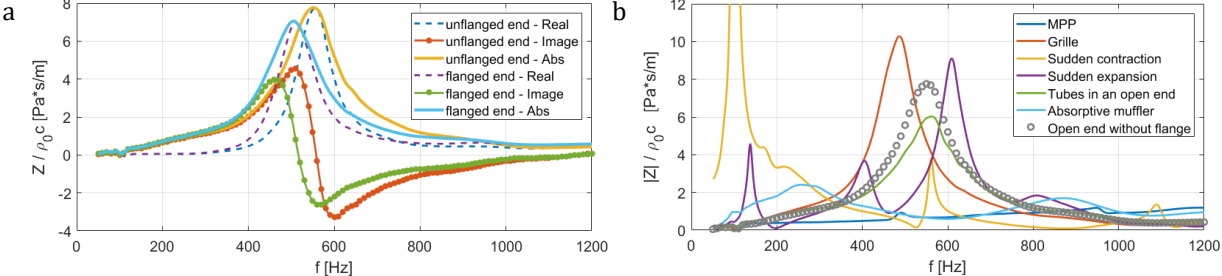
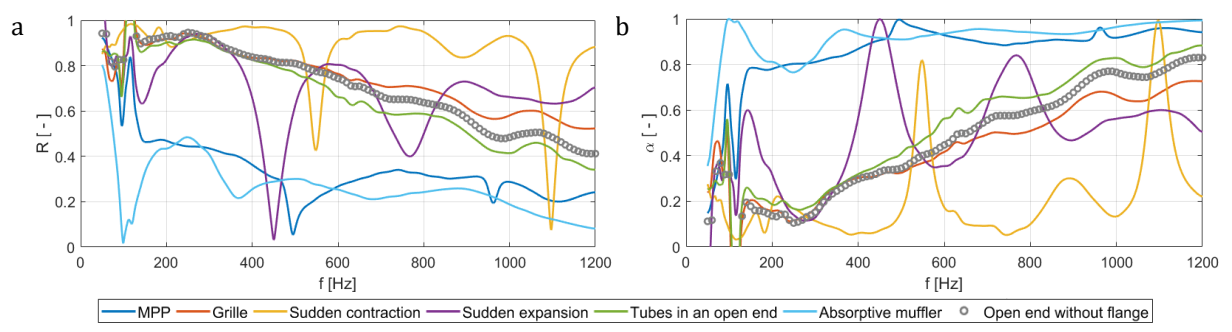


Figure 6. Measured open end impedance: a) unflanged and flanged, b) variants V1-V8.

The following figures (Figure 7) show a comparison of the reflection coefficient R and, for the convenience of interpretation, the absorption coefficient  $\alpha$  for different variants (V1-V7) of the waveguide termination. Absorption and, consequently, reflection of an acoustic wave is related not only to the wave absorbed by the termination of the waveguide forming the acoustic system, e.g. a muffler, but also to the wave emitted by the open outlet of the waveguide. It can be seen that when the normalized value of the termination impedance  $|Z|/\rho_0 c$  oscillates around the value of 1 Pa·s/m, it may mean matching to the characteristic impedance of the medium  $\rho_0 c$ , which results in an increased sound absorption value.



**Figure 7.** Measured values of coefficients for variants V1-V7: a) reflection coefficient, b) absorption coefficient.

It can be seen that both the presence of a standard ventilation grille and the tubes placed inside the waveguide outlet do not significantly change the parameters of the wave reflected and radiated by the waveguide outlet compared to the open end without modification.

According to Eq. (7), the radiation impedance of the acoustic wave through an open outlet with and without a flange was determined. The radiation impedance values were compared with the values calculated theoretically according to Eq. (5)-(6) and numerically using the finite element method (Figure 8).

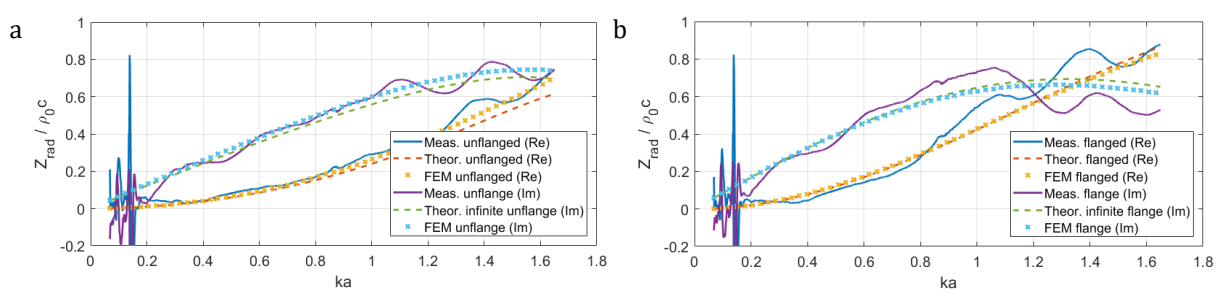
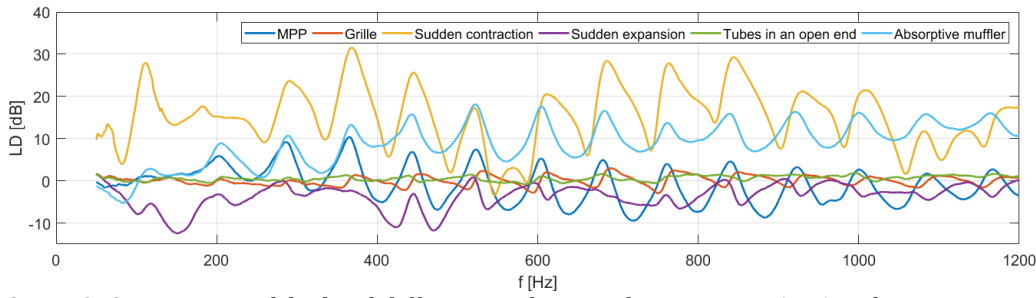


Figure 8. Comparison of radiation impedance: a) unflanged open end, b) flanged open end.

The sound pressure level of the wave radiated by the individual waveguide outlet modification variants was measured using an additional microphone located 1 m from the outlet. The assessment of the noise generated by the outlet was performed using the LD (Level Difference) parameter, which is analogous to the IL (Insertion Loss) parameter, but in this case, due to the different length of the measuring setup for the individual variants, it is not appropriate. The Figure 9 shows the differences in the sound pressure level values of the individual variants in relation to the open outlet without modification. Negative values indicate a higher  $L_p$  value

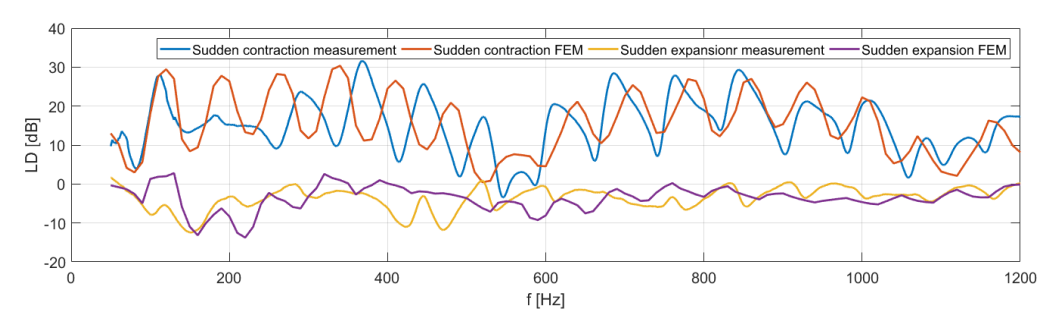
$$LD = L_v - L_o, (10)$$

where  $L_v$  – acoustic pressure level of analyzed variant,  $L_o$  – acoustic pressure level of open end.



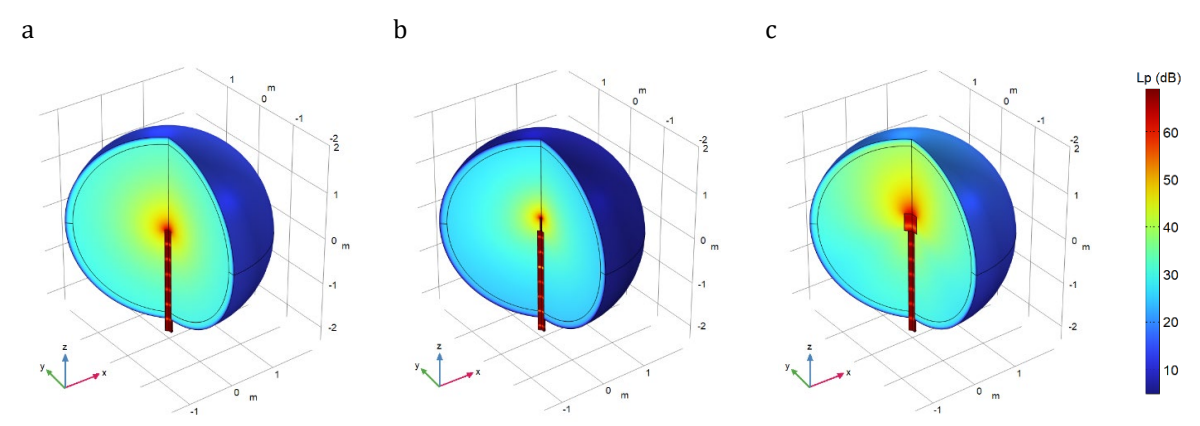
**Figure 9.** Comparison of the level difference values *LD* for variants V1-V6 with respect to V7.

Figure 10 shows comparisons of measured values  $L_p$  with those calculated using FEM for simple modifications of the outlet geometry (V3 and V4).



**Figure 10.** Comparison of the levels difference values *LD* of the FEM and measurement for variants V3 and V4.

The sound pressure level distribution calculated using FEM is presented below (Figure 11), which confirms the experimental results obtained for a simple modification of the waveguide outlet geometry.



**Figure 11.** FEM simulations of the sound pressure level Lp of the wave radiated by different waveguide ends: a) open end, b) sudden contraction, c) sudden expansion.

## 6. Conclusions

A measurement setup was designed and constructed to enable measurement of the waveguide outlet end impedance based on the transfer function. A two-step verification of the measuring setup was carried out.

The influence of the flange on the open end impedance as well as the radiation impedance of the waveguide outlet was experimentally confirmed. The measured radiation impedance values were compared with numerical and theoretical calculations, obtaining similar values (Figure 8).

Seven variants of waveguide open end modification were tested to verify the sound pressure level changes. According to the energy conservation law, the energy of the absorbed wave is related to the energy of the wave dissipated in some termination structures and the energy of the transmitted wave. The comparison of these two parameters allows us to determine which part of the acoustic wave was actually absorbed and which part was radiated by the termination of the waveguide.

A comparison of Figure 7 and Figure 9 shows that the variant of the waveguide outlet modification consisting in placing several dozen tubes of different lengths inside, does not significantly affect the wave reflected from such an outlet or the wave radiated to the environment. Similar slight differences are visible for the variant of the outlet with a ventilation grille.

The waveguide termination in the form of an MPP muffler shows absorption in the low frequency range, i.e. up to 380 Hz. Above a frequency of about 380 Hz, the values of the sound pressure level difference *LD* oscillate close to zero, which marginalizes the impact of this type of modification in this frequency range. A more effective solution in terms of reducing the noise emitted by the waveguide outlet in the entire range of analyzed frequencies is an absorption muffler, reducing the sound pressure level of the radiated wave by about 10 dB for frequencies above 380 Hz and for frequencies below 380 Hz similarly to the MPP muffler (Figure 9).

Among the analyzed variants, the most effective solution in terms of limiting the wave emitted by the waveguide outlet to the environment is the modification by means of sudden contraction. In this case, the

absorption of the acoustic wave does not reach high values because the rigid surface inside the waveguide cross-section causes significant reflection. However, due to the high reflection values, the wave emitted to the environment has the smallest amplitude among the analyzed solutions. It is worth noting that taking into account the flow of the medium often present in ventilation systems, these reflective structures can affect both the flow and the total noise in different ways.

In summary, the most effective variant in terms of the acoustic wave emitted by the open outlet to the environment is the modification of the outlet in the form of a sudden contraction. However, this solution does not reduce the noise inside the waveguide. Therefore, the best solution is the one for which there is both the highest absorption value and the highest value of the difference in the level of the wave emitted by the outlet. Such a variant is the use of an absorption muffler at the waveguide outlet.

## Additional information

The author declare: no competing financial interests and that all material taken from other sources (including their own published works) is clearly cited and that appropriate permits are obtained.

#### References

- 1. F. Fahy; Foundations of Engineering Acoustics; Elsevier, 2003
- 2. L. E. Kinsler, A. R. Frey, A. B. Coppens, and J. V. Sanders; Fundamentals of Acoustics; John Wiley & Sons, Inc., 2000
- 3. A. D. Pierce; An Introduction to Its Physical Principles and Applications; 2019
- 4. A. Snakowska, J. Jurkiewicz; Efficiency of energy radiation from an unflanged cylindrical duct in case of multimode excitation; Acta Acust. united with Acust., 2010, 96 (3), 416–424; DOI: 10.3813/AAA.918294
- 5. A. Snakowska, H. Idczak, B. Bogusz; Modal analysis of the acoustic field radiated from an unflanged cylindrical duct Theory and measurement, Acta Acust. united with Acust., 1996, 82 (2), 201–206
- 6. D. T. Blackstock; Fundamentals of Physical Acoustics; Wiley-Interscience; 2000
- 7. X. X. Chen, X. Zhang, C. L. Morfey, P. A. Nelson; A numerical method for computation of sound radiation from an unflanged duct; J. Sound Vib., 2004, 270 (3), 573–586; DOI: 10.1016/j.jsv.2003.09.055
- 8. J.-P. Dalmont, C. J. Nederveen, N. Joly; Radiation impedance of tubes with different flanges: numerical and experimental investigations; J. Sound Vib., 2001, 244 (3), 505–534; DOI: 10.1006/jsvi.2000.3487
- 9. S. Dykas, W. Wróblewski, S. Rulik, T. Chmielniak; Numerical Method for Modeling of Acoustic Waves Propagation; Arch. Acoust., 2010, 35 (1), 35–48; DOI: 10.2478/v10168-010-0003-7
- 10. S. Lidoine, H. Batard, S. Troyes, A. Delnevo, M. Roger; Acoustic radiation modelling of aeroengine intake comparison between analytical and numerical methods; 7th AIAA/CEAS Aeroacoustics Conference and Exhibit, Maastricht, Netherlands, 28-30 May, 2001; DOI:10.2514/6.2001-2140
- 11. S. Marburg, B. Nolte; Computational Acoustics of Noise Propagation in Fluids Finite and Boundary Element Methods; Springer Berlin Heidelberg, 2008
- 12. M. L. Munjal; Acoustics of ducts and mufflers; John Wiley & Sons, 2014
- 13. D. Marx, F. Margnat, H. Bailliet, C. Prax, Z. Qiu, J.-C. Valière; Uncoupled multimodal wave reflection from guide termination with different flanges: Experimental and numerical investigation; Acta Acust., 2024, 8 (38), 1-13; DOI: 10.1051/aacus/2024015
- 14. D. Maa; Potential of microperforated panel absorber; J. Acoust. Soc. Am., 1998, 104, 2861–2866; DOI: 10.1121/1.423870
- 15. N. Hiremath, V. Kumar, N. Motahari, D. Shukla; An Overview of Acoustic Impedance Measurement Techniques and Future Prospects; Metrology, 2021, 1 (1), 17–38; DOI: 10.3390/metrology1010002.
- 16. J. W. S. B. Rayleigh, The theory of sound, vol. 2. Macmillan, 1896
- 17. H. Levine, J. Schwinger; On the radiation of sound from an unflanged circular pipe; Phys. Rev., 1948, 73 (4), 383–406; DOI: 10.1103/PhysRev.73.383
- 18. M. Atig, J.-P. Dalmont, J. Gilbert; Termination impedance of open-ended cylindrical tubes at high sound pressure level; Comptes Rendus Mécanique, 2004, 332 (4), 299–304; DOI: 10.1016/j.crme.2004.02.008
- 19. ISO 10534-2:2023; Acoustics—Determination of acoustic properties in impedance tubes. Part 2: Two-microphone technique for normal sound absorption coefficient and normal surface impedance, 2023

© **2025 by the Authors.** Licensee Poznan University of Technology (Poznan, Poland). This article is an open access article distributed under the terms and conditions of the Creative Commons Attribution (CC BY) license (http://creativecommons.org/licenses/by/4.0/).